ORIGINAL ARTICLE

Mutations in *MYO1H* cause a recessive form of central hypoventilation with autonomic dysfunction

Malte Spielmann,[1,2] Luis R Hernandez-Miranda,[3] Isabella Ceccherini,[4] Debra E Weese-Mayer,[5,6] Bjørt K Kragesteen,[1] Izabela Harabula,[1] Peter Krawitz,[2] Carmen Birchmeier,[3] Norma Leonard,[7] Stefan Mundlos[1,2]

► Additional material is published online only. To view please visit the journal online (http://dx.doi.org/10.1136/jmedgenet-2017-104765).

[1]Max-Planck-Institute for Molecular Genetics, Berlin, Germany
[2]Institute for Medical Genetics and Human Genetics, Charité Universitätsmedizin Berlin, Berlin, Germany
[3]Max-Delbrück-Centrum für Molekulare Medizin in der Helmholtz-Gemeinschaft, Germany
[4]UOC Genetica Medica, Istituto G Gaslini, Genova, Italy
[5]Center for Autonomic Medicine in Pediatrics (CAMP), Ann & Robert H. Lurie Children's Hospital of Chicago, Stanley Manne Children's Research Institute, Chicago, Illinois, USA
[6]Northwestern University Feinberg School of Medicine, Chicago, Illinois, USA
[7]Department of Medical Genetics, University of Alberta, Edmonton, Canada

Correspondence to
Stefan Mundlos, Max-Planck-Institute for Molecular Genetics, Ihnestraße 63-73, 14195 Berlin, Germany ; mundlos@molgen.mpg.de

MS and LRH-M contributed equally.

Received 26 April 2017
Revised 14 June 2017
Accepted 16 June 2017
Published Online First 7 August 2017

To cite: Spielmann M, Hernandez-Miranda LR, Ceccherini I, *et al*. *J Med Genet* 2017;**54**:754–761.

ABSTRACT

Background Congenital central hypoventilation syndrome (CCHS) is a rare life-threatening disorder of respiratory and autonomic regulation. It is classically caused by dominant mutations in the transcription factor *PHOX2B*. The objective of the present study was to identify the molecular cause of a recessive form of central hypoventilation with autonomic dysfunction.

Methods Here, we used homozygosity mapping and whole-genome sequencing in a consanguineous family with CCHS in combination with functional analyses in CRISPR/Cas9 engineered mice.

Results We report on a consanguineous family with three affected children, all tested *PHOX2B* mutation negative, presenting with alveolar hypoventilation and symptoms of autonomic dysregulation. Whole-genome sequencing revealed a homozygous frameshift mutation in exon 25 of the *MYO1H* gene (c.2524_2524delA) segregating with the phenotype in the family. *MYO1H* encodes for the unconventional myosin IH, which is thought to function as a motor protein in intracellular transport and vesicle trafficking. We show that *Myo1h* is broadly expressed in the mouse lower medulla, including the CO_2-sensitive Phox2b+ retrotrapezoid neurons. To test the pathogenicity of the variant, we engineered two *Myo1h* mutant mouse strains: the first strain (*Myo1h**) resembling the human mutation and the second being a full knock-out ($Myo1h^{FS}$). Whole-body plethysmography studies in *Myo1h** newborns with the re-engineered human mutation revealed hypoventilation and a blunted response to CO_2, recapitulating the breathing phenotype observed in the kindred.

Conclusions Our results identify *MYO1H* as an important gene in CO_2 sensitivity and respiratory control and as the cause of a rare recessive form of congenital central hypoventilation.

INTRODUCTION

Congenital central hypoventilation syndrome (CCHS, OMIM: 209880; also known as 'Ondine's curse') is a rare life-threatening autosomal disorder of respiratory and autonomic regulation.[1] CCHS classically manifests in the neonatal period and is characterised by alveolar hypoventilation during sleep. A subset of affected children also hypoventilate awake. Cessation of breathing or apnoea is less typical in CCHS than the apparent hypoventilation. Patients with CCHS require lifelong artificial ventilation. The most salient aspect of this respiratory control disorder is the inability to adjust breathing in response to changing levels of blood gases, that is, hypercapnia (high levels of CO_2) and hypoxaemia (low levels of O_2).[2] The respiratory phenotype is characteristically associated with physiological manifestations of autonomic nervous system dysregulation[3 4] as well as anatomical manifestations including Hirschsprung disease (a rare disorder that produces aganglionosis of the distal hindgut) and neural-crest tumours such as neuroblastomas, ganglioneuromas and ganglioneuroblastomas.[5 6] Dominant mutations in the paired like homeobox 2b (*PHOX2B*) gene were identified as the most common cause for CCHS.[5–7] The vast majority of individuals with CCHS are heterozygous for an abnormal expansion of a polyalanine repeat sequence (polyalanine repeat expansion mutations in exon 3 of the *PHOX2B*).[5–8] In the remaining CCHS patients, other distinct non-polyalanine repeat expansion mutations have also been found in the *PHOX2B* gene.[5–8] Most *PHOX2B* mutations occur de novo, but up to 25% of families have somatic mutations and only very few familial cases of CCHS have germline mosaicism.[7 9 10]

Here, we report on a consanguineous family with three CCHS-related *PHOX2B* mutation-negative children, all presenting with alveolar hypoventilation, apnoea and bradycardia and various manifestations of autonomic nervous system dysregulation. We identified a homozygous frameshift mutation in the *MYO1H* gene in the three affected infants. In mice, *Myo1h* is broadly expressed in the lower medulla including Phox2b+ neurons of the retrotrapezoid nucleus. These neurons are CO_2 sensitive and have been reported absent in mice carrying the most frequent human *PHOX2B* mutation ($Phox2b^{27ala/+}$), which interferes with normal response to hypercapnia.[11] To investigate the potential role of *Myo1h* in the regulation of breathing, we mutated *Myo1h* in mice by CRISPR/Cas9 genome editing. Mice with the re-engineered human mutation (*Myo1h** mice) showed severe hypoventilation and blunted response to CO_2, recapitulating the hypoventilation phenotype observed in patients. Collectively, our data identified *MYO1H* as an important player in respiratory control and a cause of a novel recessive form of congenital hypoventilation.

Methods

Subjects and ethics approval

The study was performed with the approval of the Charité Ethics Committee, Berlin, Germany. Patients were enrolled with written informed consent for participation in the study. The clinical evaluation included medical history interviews, a physical examination and review of medical records. Blood samples or buccal swaps were obtained from each participating individual, and DNA was extracted by standard procedures.

SNP array genotyping and homozygosity mapping

We performed a genome-wide linkage analysis with homozygosity mapping by using Affymetrix Genome-Wide Human SNP 6.0 arrays and genomic DNA samples from seven members of the family, namely, the three affected individuals IV:1, IV:2 and IV:3 as well as the unaffected individuals III:1, III:2, IV:4 and IV:5. Homozygosity mapping was performed as described.[12]

Whole-genome sequencing

Whole-genome sequencing was performed in individual IV:3. Briefly, genomic DNA was sequenced on an Illumina HiSeq 2000 Sequencer via a paired-end 100 bp protocol.[13 14] Primary data were filtered according to signal purity by the Illumina Realtime Analysis software V.1.8. Subsequently, the reads were mapped to the human genome reference build GRCh37/hg19 (http://www.genome.ucsc.edu/) using the Burrows-Wheeler Aligner's Smith-Waterman Alignment (BWA-SW) algorithm. Mean coverage was 100× in the exome, and 95.6% and 86.4% of target bases were covered more than 10× and 30×, respectively. Further annotation and filtering for high-quality rare variants (minor allele frequency <0.1%) with a predicted impact on protein sequence or splicing were performed as described.[15]

Sanger sequencing

Validation and cosegregation analyses were performed by Sanger sequencing on an ABI 3730 DNA Analyzer with BigDye chemistry V.3.1.

CRISPR/Cas9 single guide RNA (sgRNA) selection and cloning

sgRNAs were designed to induce point mutations or flanking the regions to re-arrange. We used the http://crispr.mit.edu/ platform to obtain candidate sgRNA sequences with little off-target specificity. Complementary strands were annealed, phosphorylated and cloned into the BbsI site of pX459 or pX330 CRISPR/Cas9 vector (CRISPR sgRNA sequences are listed in online Supplemental table 3).

Embryonic stem (ES) cell culture and transfection

A total of 300 000 G4 cells (129xC57BL/6 F1 hybrid ES cells) were seeded on CD-1 feeders and transfected with 8 µg of each CRISPR construct using FuGENE technology (Promega). When the construct originated from the pX330, vector cells were cotransfected with a puromycine-resistant plasmid. PX459 in contrast already contains a puromycine-resistant cassette. After 24 hours, cells were split and transferred onto DR4 puromycine-resistant feeders and selected with puromycine for 2 days. Clones were then grown for 5–6 more days, picked and transferred into 96-well plates on CD-1 feeders. After 2 days of culture, plates were split in triplicates, two for freezing and one for growth and DNA harvesting. Positive clones identified by PCR or Sanger sequencing were thawed and grown on CD-1 feeders until they reached an average of 4 million cells. Three vials were frozen, and DNA was harvested from the rest of the cells to confirm genotyping. PCR-based genotyping was performed as previously described.[16]

To create a mutation in exon 25 of both *Myo1h* isoforms, we designed one sgRNA in exon 25 as close as possible to the mutation observed in the family. We detected compound and homozygous mutations in at least 73 clones (out of 96) and selected two clones with homozygous frameshift mutations in exon 25 for tetraploid ES cell aggregation. We also identified one heterozygous frameshift mutation. To create a complete knock-out of *Myo1h*, we designed one sgRNA in exon 3.

Es cell aggregation

A frozen ES cell phial was seeded on CD-1 feeders, and cells were grown for 2 days. Mice were generated by diploid or tetraploid ES cell aggregation.[17] All animal procedures were in accordance with institutional, state and government regulations (Berlin: LAGeSo).

In situ hybridisation and immunohistochemistry

In situ hybridisation for *Myo1h* was carried out on wild-type (WT) embryos (C57/Bl6J) at birth as previously described.[18] Primers use to make Myo1h in situ probes are as follows: Myo1h-S-F: TTCATTCGATTCCCCAGAACCC and Myo1h-S-R: CTC AGCAGATTGGAAGCATTT. Immunocytochemistry was carried out on WT and *Myo1h** using the following primary antibodies: rabbit anti-Nk1R (Sigma, catalogue No S8305), guinea pig and rabbit anti-Phox2b (kindly provided by JF Brunet, Ecole Normale Superieure, Paris), and guinea pig anti-Islet1/2 (kindly provided by T Jessell, Columbia University, New York). Pre-Bötzinger and retrotrapezoid neurons were systematically quantified in 20-µm-thick consecutive sections using facial and ambiguus motor neurons as landmarks.

Quantitative real-time PCR analysis

RNA from control mice was isolated using TRIzol (Invitrogen) in accordance with the manufacturer's instructions. cDNA was synthesised using SuperScript III (Invitrogen). Real-time PCR was performed with Absolute qPCR SYBR Green mix (AbGene) on a Biorad C1000 Thermal cycler. Threshold cycle values were normalised against the housekeeping gene Ube2l3. The following primers were used: Ube2l3_Forward:GGTCTGTCTGCCAGT CATTAGTGC, Ube2l3_Reverse: GGGTCATTCACCAGT GCTATGAG, Myo1h_Forward: AGTTCGTAGTGCTTGT-GAGG and Myo1h_Reverse: GTATGCTGACCTCTGTGTG.

Plethysmography

Unrestrained whole-body plethysmography was performed using a self-build plethysmograph specifically designed for breathing analysis of newborn mice.[19] It consists of a 20 mL Plexiglas chamber and attached to a pressure transducer that is particularly sensitive (Validyne DP103-10, Northridge, California, USA). The chamber was also connected to a Hamilton syringe for pressure calibrations. Plethysmographic recordings were analysed on Elphy software (developed by G Sadoc at CNRS, Gif-sur-Yvette, France). For CO_2 challenges, a gas mixture was composed of 8% CO_2 and 21% O_2, and 71%$_{N2}$ was applied into the chamber.

RESULTS

Family pedigree and clinical phenotype of affected subjects

Five children born to parents with native American background were included in the cohort. Three of the children (IV:1, IV:2 and IV:3) demonstrated an autosomal recessive pattern of alveolar hypoventilation in the neonatal period characterised by

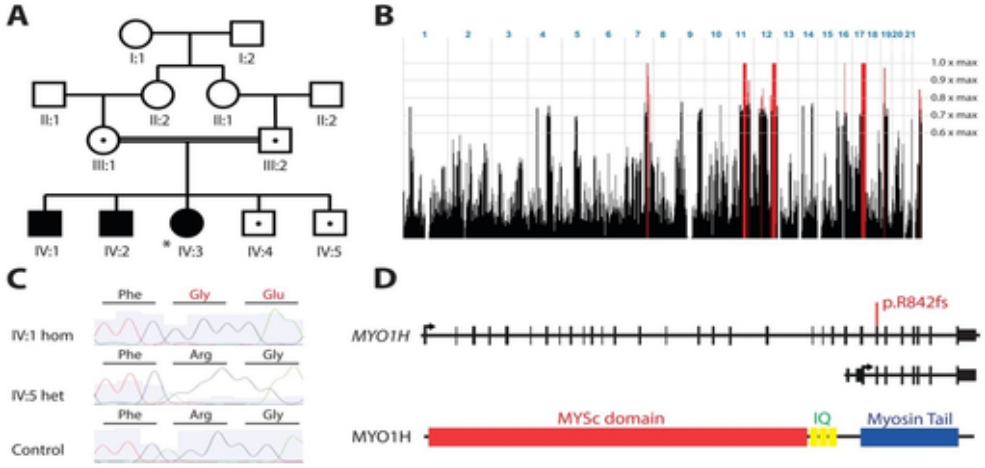

Figure 1 A recessive variant of *MYO1H* is associated with alveolar hypoventilation, apnoea and bradycardia.(A) Pedigree of the family investigated. Black symbols indicate individuals affected with alveolar hypoventilation. Homozygosity mapping was performed in individuals III:1, III:2 and IV:1–5, and whole-genome sequencing was performed with DNA from individual IV:3 designated with an asterisk (*). (B) Representation of genome-wide homozygosity in the family following SNP array genotyping with 250k arrays. Homozygosity regions are plotted against the physical position genome wide. Homozygosity regions on chromosomes 7, 11, 12, 16 and 17 are indicated by the red peaks. (C) All affected individuals carried the homozygous frameshift mutation c.2524_2524delA (p.R842Gfs*11) in *MYO1H* on chromosome 12q24.11. Parents and healthy siblings were heterozygous for the variant, which was absent in healthy controls. (D) *MYO1H* encodes for the unconventional myosin IH, which is thought to serve in intracellular movements and vesicle trafficking. It consists of a well-conserved myosin head (MYCs domain), three short calmodulin-binding motifs (IQ) and a highly specific tail (myosin tail). The frameshift mutation p.R842Gfs*11 is predicted to result in a truncated protein missing the myosin tail or in a complete loss of function induced by in non-sense mediated decay.

shallow breathing and apnoea, necessitating mechanical ventilation during sleep (figure 1A; online Supplemental figure 1). Additionally, all three affected infants had feeding difficulties from the neonatal period with gastro-oesophageal reflux, aspiration, autonomic features of oesophageal and intestinal dysmotility, as well as achalasia leading to feeding by gastrostomy and jejunostomy tubes. Two of the infants progressed to recurrent central apnoea while awake or asleep, and all three lacked ventilatory response to high levels of CO_2, necessitating tracheostomy and artificial ventilation as life support.

Individual IV:1 presented with respiratory symptoms at 5 months of age. He was well at birth with reported 'blue spells' at home for which medical care was not sought. He was admitted to the ward with respiratory symptoms for supportive care where he subsequently had a cardiac arrest and later placed on extra-corporeal membrane oxygenation for stabilisation. At 6 months of age, he underwent tracheostomy and gastrostomy tube placement as he failed to improve with respect to ventilation. He died in the paediatric intensive care unit at 11 months of age after unsuccessful resuscitation with another cardiac arrest. No autopsy was performed.

Individual IV:2 was delivered by caesarean section for non-reassuring heart rate with Apgar scores of 8 at 1 min and 9 at 5 min with mild oxygen desaturations after birth. He underwent a polysomnography at 18 days of age, which showed a mean end-tidal carbon dioxide of 32 mm Hg with a peak of 40 mm Hg and mean pulse oxygen saturation of 98% with a nadir of 86%. He had a normal ECG. Oesophageal dysmotility and achalasia were documented on barium swallow with a normal endoscopy, and a head MRI showed no structural abnormalities. He was discharged home at 1 month and returned to hospital 2 weeks later with symptoms of bronchiolitis. Polysomnography during this admission showed a mean end-tidal carbon dioxide of 48 mm Hg with a peak of 55 mm Hg and mean pulse oxygen saturation of 96% with a nadir of 85%. It was determined that he had swallowing dysfunction and aspiration risk so he was discharge home after a gastrostomy tube was placed. Deterioration in respiratory parameters was documented by polysomnography at 2 months with parameters at 5 months showing a mean end-tidal carbon dioxide of 88 mm Hg with a peak of 95 mm Hg and mean pulse oxygen saturation of 92% with a nadir of 69%. After a trial of non-invasive ventilation with bilevel positive airway pressure, he underwent tracheostomy and started on nocturnal ventilation at 14 months. Gastrostomy tube was placed because of swallowing dysfunction and aspiration. He was noted to be hypotonic and areflexic. At 8 years of age, he remains on nocturnal ventilation, is able to walk with support and attends school in a programme modified for his global developmental delay. A seizure disorder was identified at 4 years of age, which is well controlled on antiepileptic medications.

Individual IV:3 presented at 5 months of age with bronchiolitis requiring intubation and ventilation with a 15-day admission to the paediatric intensive care unit. After discharge to the ward, she was noted to have apnoea, instability in both respiratory and heart rates, and dynamic muscle tone; 4 days after transfer to the ward, she suffered a cardiorespiratory arrest requiring 4 min of cardiopulmonary resuscitation. She was extubated on several occasions with progressively shorter intervals before requiring reintubation for central hypoventilation and apnoea. At 7 months, a tracheostomy tube was placed for long-term ventilation. She had normal MRI of the head and brainstem, normal nerve conduction studies and a normal muscle biopsy. Auditory brain responses and EEG showed no abnormalities. Signs of autonomic dysregulation were prominent with sinus bradycardia, temperature dysregulation, bladder dysfunction requiring chronic catheterisation and gastrointestinal dysmotility resulting in gastro-oesophageal reflux and chronic constipation. Swallowing dysfunction necessitated gastrostomy tube placement for feeding and eventually gastro-jejunal feeding with ongoing failure to thrive. She

had transient pulmonary hypertension with pulmonary hypertensive crises as well as breath-holding spells that resolved in the first year of life. Her clinical course was complicated by variable lymphocyte numbers and low lymphocyte responses potentially contributing to recurrent bacterial and viral infections. She was discharge from hospital at 3. 5 years of age. At 15 years of age, she is on continuous ventilation with severe kyphoscoliosis, myopathy and a restrictive lung disease with a forced vital capacity of 20% of her predicted and developed a seizure disorder in the last year. She is able to walk short distances and attends school in a programme modified for her global developmental delay. She also had mild bilateral strabismus, myopia and astigmatism.

Individual IV:4 was diagnosed at 2.5 months of age with regurgitation of feeds and cough. He was hospitalised for increased work of breathing but did not require oxygen during the admission. He was confirmed to have swallowing dysfunction. He experienced subsequent hospitalisations for aspiration pneumonia with no admissions to the intensive care unit. Overnight oximetry recording showed no evidence of oxygen desaturation, but polysomnography was not performed. He is now 12 years of age with his most recently admission to hospital at 8 years of age; a venous carbon dioxide during that admission was 23 mm Hg. Individual IV:5 is alive and well at 17 years of age with no health concerns.

Homozygosity mapping and whole-genome sequencing identified a variant in *MYO1H*

Because of overt hypoventilation in the three affected infants and concern for diagnosis of an atypical form of CCHS, *PHOX2B* testing was performed by Sanger sequencing, microsatellite analysis and multiplex ligation-dependent probe amplification—although no CCHS-related mutations were identified. We therefore performed homozygosity mapping by SNP array genotyping and identified five homozygous regions on chromosomes 7, 11, 12, 16 and 17 (figure 1B and online Supplemental table 1).

After whole-genome sequencing of one affected individual (IV:3) and filtering for rare potentially damaging variants, we detected six homozygous missense and one frameshift variants in the homozygous regions. Sanger sequencing of the entire family confirmed that all variants cosegregated with the phenotype, but only two missense variants and the frameshift variant were

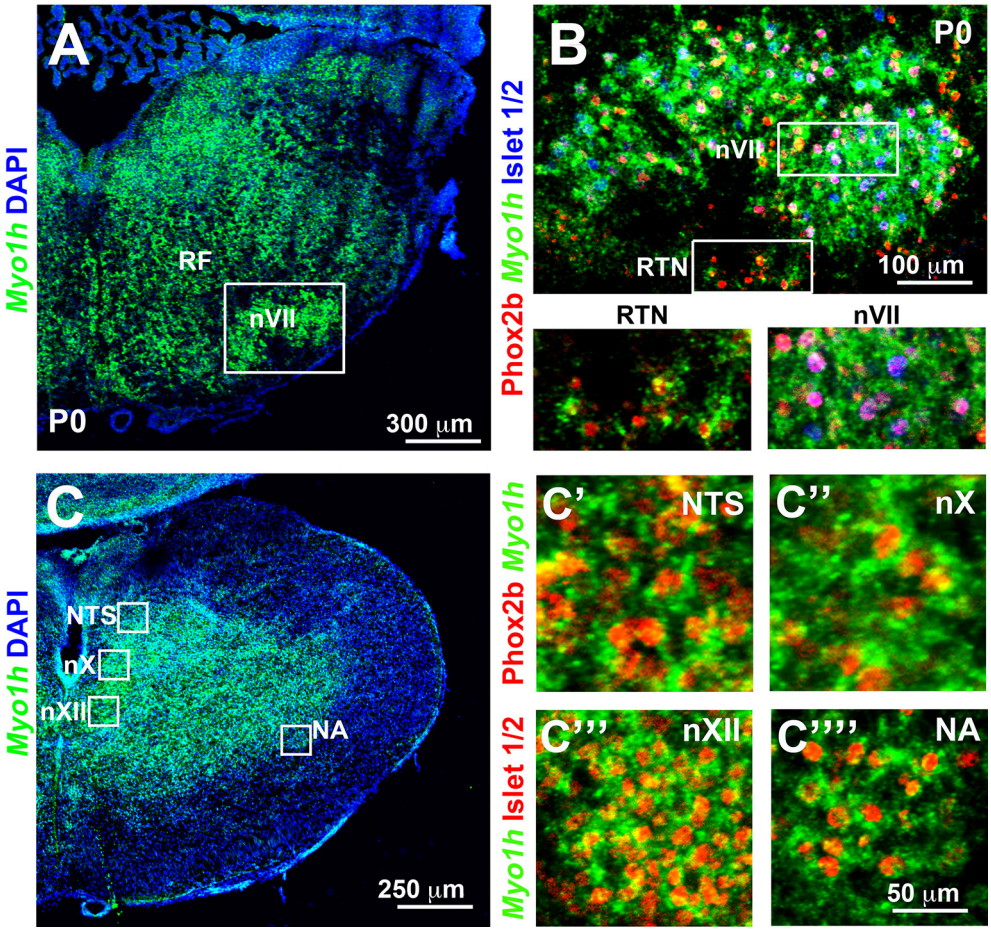

Figure 2 Expression of *Myo1h* in newborn mice. (A, C) In situ hybridisation for *Myo1h* (green) on different rostral–caudal levels of the lower medulla of wild-type newborn mice. Sections were counterstained with 4′,6-diamidino-2-phenylindole (DAPI) (blue). (A) *Myo1h* is expressed throughout the reticular formation (RF) and highly expressed in the facial motor nucleus (nVII). (B) Magnification of the boxed area in A, showing *Myo1h* transcripts and in addition Islet1/2+ (blue) and Phox2b+ (red) immunohistological signals. Motor neurons of the facial nucleus (nVII) coexpress *Myo1h*, Islet1/2+ and Phox2b+, whereas a subpopulation of retrotrapezoid neurons (RTN) coexpress *Myo1h* and Phox2b. (B′B″) Magnifications of the boxed areas in B. (C) *Myo1h* transcripts in the nucleus of the solitary tract (NTS) as well as in the vagal (nX), hypoglossal (nXII) and ambiguus (NA) motor nuclei. (C′C″) Magnifications of the boxed areas in C showing *Myo1h* transcripts and in addition Phox2b (red) immunohistological signals in the NTS and nX. (C‴C⁗) Magnification of the boxed areas in C showing *Myo1h* transcripts and in addition Islet1/2+ (red) neurons in nXII and NA.

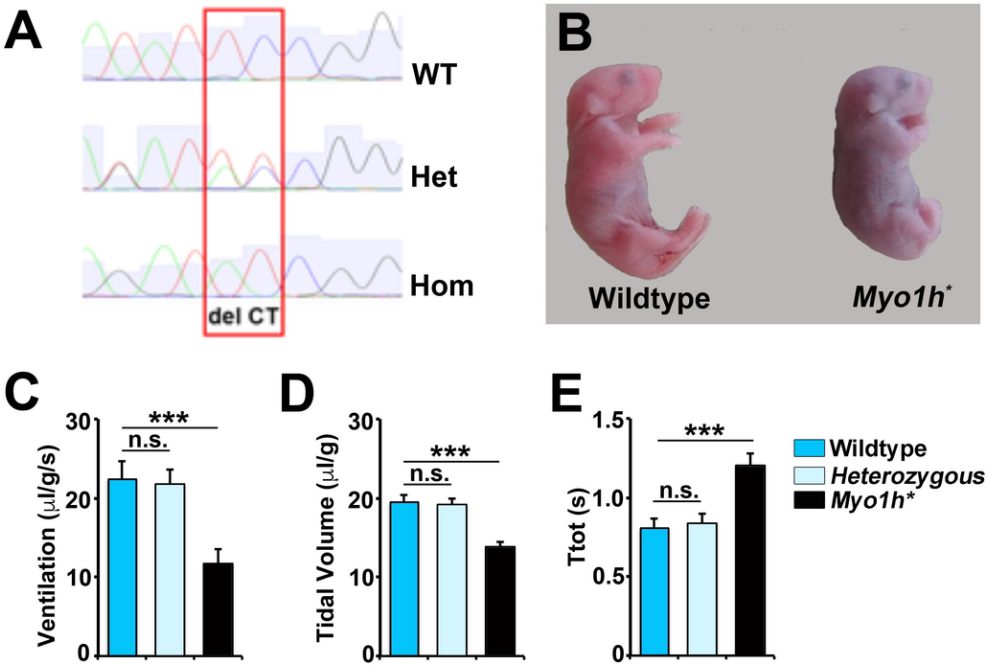

Figure 3 Hypoventilation in *Myo1h** newborn mice. (A) Generation of a mouse model harbouring a frameshift mutation in exon 25 of the *Myo1h* gene by CRISPR/Cas9 genome editing; the mutation is similar to that identified in patients. (B) Pups carrying the homozygous frameshift mutation (*Myo1h**) displayed strong cyanosis at birth. (C–E) Overall ventilation, tidal volume and Ttot (cycle length duration) of wild-type (n=3), heterozygous (n=6) and *Myo1h** (n=6) mutants at birth. ***p<0.0001 (one-way analysis of variance (ANOVA)). n.s., non-significant (p>0.05, one-way ANOVA).

predicted to be damaging and absent or very rare in controls cohorts such as Exome Aggregation Consortium (ExAC) and 1000 genomes (online Supplemental figure 1 and Supplemental table 2). We detected missense variants in *LPO* (p.R452H) and in *TBX4* (p.V218M). LPO encodes for a lactoperoxidase, which is secreted from mammary, salivary and other mucosal glands. Inactivation in mice results in abnormalities of lens development.[20] The variant p.R452H in LPO is present in 63 healthy individuals listed in the ExAC database. *TBX4* is a transcription factor with important functions in limb development. During development, it is specifically expressed in the hindlimb, and inactivation in mice results in abnormal limbs.[20 21] Mutations in *TBX4* have been reported in patients with ischiocoxopodopatellar (small patella) syndrome (MIM#147891) and childhood-onset pulmonary arterial hypertension. In addition, *TBX4* including overlapping deletions of 17q23.2 has previously been shown to associate with with childhood-onset pulmonary arterial hypertension.[22–24] The heterozygous mutation p.V218M in *TBX4* is present in 14 healthy individuals listed in the ExAC database. Even though no limb abnormalities were observed in the family presented here, it needs to be considered that the variant in *TBX4* (p.V218M) could also contribute to the phenotype. The homozygous frameshift mutation c.2524_2524delA in *MYO1H* (p.R842Gfs*11; chr12:109879453_109879453delA) was present in all affected individuals. Their parents (III:1 and III:2) and the two unaffected siblings (IV:4 and IV:5) were heterozygous for the variant, and it was absent in healthy unrelated control individuals (figure 1C, D; online Supplemental figure 1).

Evaluation of *Myo1h* gene function in mice

Given that *Myo1h* did not have a known function in nervous system development, we analysed the expression of *Myo1h* in newborn WT mice by quantitative RT-PCR and in situ hybridisation. At birth, *Myo1h* was highly expressed in the central nervous system, including the forebrain, midbrain and lower medulla (online Supplemental figure 2). In the lower medulla, *Myo1h* was broadly expressed throughout the reticular formation (figure 2). Interestingly, transcripts were detected in Phox2b+ neurons of the retrotrapezoid nucleus and the nucleus of the solitary tract, as well as motor neurons of the facial, vagal and ambiguus nuclei (figure 2). The retrotrapezoid nucleus and the nucleus of the solitary tract play important roles in breathing.[25] We thus reasoned that *MYO1H* was a plausible candidate gene to be causal of unexplained alveolar hypoventilation.

We used CRISPR/Cas9 genome editing to directly test the consequences of the detected *MYO1H* variant.[16 26 27] In the first line, named *Myo1h**, we designed a sgRNA to target exon 25 in a position similar to the identified *MYO1H* human mutation. The sgRNA was transfected into mouse ES cells together with a construct encoding the Cas9 protein. We identified several clones carrying homozygous frameshift mutations; the sequence of a *Myo1h** clone that was used to generate the mutant mice is shown in online Supplemental figure 3. This mutation is predicted to result in premature termination and non-sense mediated decay of the two mRNA isoforms produced by the *Myo1h* gene (online Supplemental figure 3). Tetraploid ES cell aggregation was performed to produce highly chimeric mice.[16 28]

All highly chimeric mice with the homozygous *Myo1h** mutation mice died in the first four postnatal hours. None of the animals had milk in the stomach, feeding was not observed. This provided the first evidence that mutations in *Myo1h* resulted in a breathing deficit. We also identified a clone with a heterozygous frameshift mutation (figure 3A) and performed tetraploid ES cell aggregation.[16 28] Heterozygous highly chimeric mice (*Myo1h*$^{*/+}$*) mice were viable and fertile and did not display any breathing deficits. Matings of heterozygous *Myo1h*$^{*/+}$ mice produced homozygous (*Myo1h***) offspring in expected Mendelian proportions (25%). Several homozygous mutant (4/12) pups displayed severe cyanosis already at birth and did not start to breathe. The remaining (8/12) animals did not display obvious

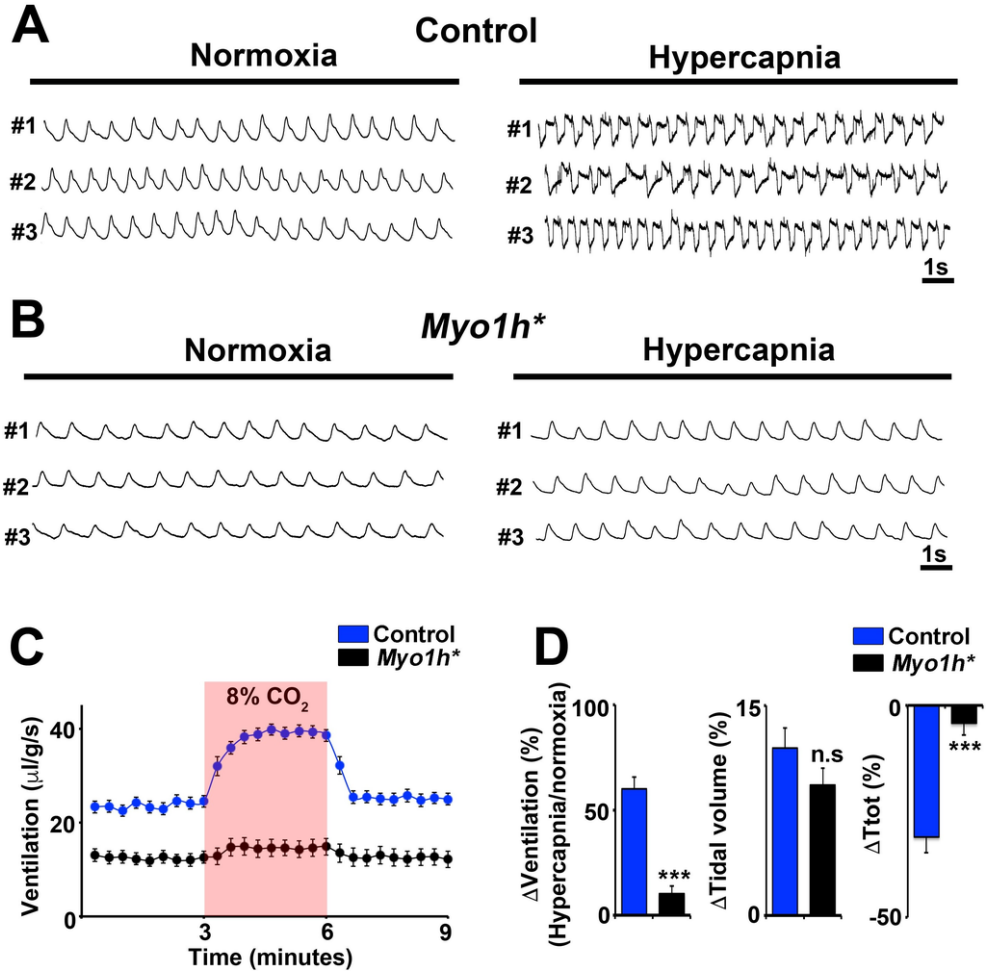

Figure 4 Blunted response to CO_2 in *Myo1h** newborn mice. (A, B) Representative plethysmographic traces of control (n=9; breathing behaviour of wild-type and heterozygous mice was indistinguishable and is shown as controls) and *Myo1h** (n=6) mice in normal air (normoxia) or in hypercapnia (8% CO_2). Numbers displayed on the left indicate distinct tested newborn mice. (C) Mean ventilation values in air or 8% CO_2 (highlighted area) in *Myo1h** mice (black circles, n=6) and control littermates (blue circles, n=9). Each circle represents the mean±SEM over a 20 s period. (D) Left, ventilatory responses to hypercapnia expressed as the percentage of ventilation change relative to the baseline of ventilation, using the formula 100×(peak ventilation−baseline ventilation)/baseline ventilation. The peak of ventilatory response to hypercapnia was determined over the entire hypercapnic exposure. Middle, percentage of tidal volume change in response to hypercapnia. Right, percentage of Ttot change in response to hypercapnia. The tidal volume and Ttot change were calculated by applying the above formula. ***p<0.0001 (two-tailed t-test). n.s., non-significant (p>0.05, two-tailed t-test).

deficits in motor behaviour (8/12), but they deteriorated soon after delivery and displayed cyanosis (figure 3B). None of the homozygous mutants fed, and they again died before the fourth postnatal hour.

Myo1h is essential for breathing control

Since all homozygous *Myo1h** mice displayed indications of severe breathing deficits, we performed plethysmographic recordings soon after delivery. We observed marked deficits in ventilatory parameters, such as longer breathing cycles and smaller tidal volumes in the mutant mice compared with control (WT and heterozygous) littermates, which led to a 46% reduction of ventilation in the mutants (figure 3C–E). Next, we assessed the capacity of homozygous *Myo1h** mice to respond to hypercapnia (high levels of CO_2). In control (WT and heterozygous) mice, a transient (30 s) exposure to 8% CO_2 in the air activates breathing by reducing the length of breathing cycles and increasing tidal volumes, thereby augmenting the ventilatory capacity (figure 4). This response is reversible, and normal ventilatory parameters are observed when CO_2 is removed. In homozygous *Myo1h** mice, exposure to CO_2 only mildly increased breathing cycle duration and tidal volume, resulting in an attenuated ventilatory response to hypercapnia (figure 4). We next evaluated whether *Myo1h** mutation impaired development of well-characterised breathing centres, the retrotrapezoid nucleus and pre-Bötzinger complex. Retrotrapezoid and pre-Bötzinger neurons were found in normal numbers in homozygous *Myo1h** when compared with control littermates (online Supplementary figure 4). We concluded that the *Myo1h** mutation in mice impairs breathing and in particular the response to hypocapnia.

Next, we assessed whether the phenotype was the result of a complete loss of function of *MYO1H*. To ensure that no functional protein is produced in the homozygous *Myo1h** mutants, we designed a sgRNA that targeted exon 3 of the *Myo1h* gene to generate a second mutant strain, called *Myo1h*^{FS}. This sgRNA produced a frameshift mutation that affected almost the entire coding sequence of the Myo1h protein. Similar to homozygous *Myo1h** mice, all homozygous *Myo1h*^{FS} mice displayed severe cyanosis and died within the first four postnatal hours (supplementary file 1) It is therefore likely that the phenotype observed

in the mutant mice as well as in the described patients with alveolar hypoventilation results from a complete loss of MYO1H function.

Mutations in *MYO1H* are not a common cause of central hypoventilation

Finally, we aimed to identify other unrelated individuals with symptoms of central hypoventilation that might harbour mutations in *MYO1H*. In a screening of 23 unrelated individuals with symptoms of central hypoventilation that were negative for *PHOX2B* testing, we did not identify any relevant change in sequence of *MYO1H* (data not shown).

DISCUSSION

Here, we report on a consanguineous family with three children who presented with alveolar hypoventilation, apnoea and bradycardia in early infancy, as well as altered intestinal motility, negative for a CCHS-related *PHOX2B* mutation. Homozygosity mapping combined with whole-genome sequencing revealed a homozygous frameshift mutation in the *MYO1H* gene that segregated with the clinical phenotype. Thus, our studies in *Myo1h* mutant mice identify *MYO1H* as an important gene in respiratory control and causative of a recessive form of alveolar hypoventilation when mutated.

The classical autosomal dominant *PHOX2B* mutation responsible for the CCHS disorder manifests in the neonatal period, typically characterised by respiratory arrest during sleep and, in more severe cases, also in hypoventilation in the awake state. It is also associated with Hirschsprung disease and neuroblastoma.[5 9] The phenotype in the kindred described here does not strictly meet the classical criteria for CCHS. The bradycardia observed in the newly identified kindred is not characteristic of CCHS, since patients with CCHS do not display bradycardia with apnoea or hypoventilation, but rather an uncoupling of heart rate and breathing. The oesophageal and intestinal dysmotility in the affected kindred was suggestive of a CCHS-related enteric phenotype, but the patients in the kindred did not have a biopsy-confirmed Hirschsprung disease and their oesophageal dysmotility never recovered despite advancing age. There were also other confounding features such as kyphoscoliosis, seizures, global developmental delay and bladder atonia that, with the exception of seizures and more modest developmental delay, have also not been described in CCHS. Thus, in addition to the phenotypes that resemble CCHS, other disorders present in the kindred are unique and might be unrelated to the hypoventilation.

MYO1H encodes for the unconventional myosin IH, which is thought to have a role in intracellular transport and vesicle trafficking.[29] It consists of a well-conserved myosin head (MYCs domain), three short calmodulin-binding motifs (IQ) and a highly specific myosin tail that diverges from the ones observed in other myosins (figure 1D). The tail is thought to bind to cargoes, for example, vesicles.[30] The frameshift mutation R842Gfs*11 is predicted to encode a protein devoid of the myosin tail and might also result in non-sense mediated decay of mRNA. The function of *MYO1H* had not been characterised previously, but related genes are known to function in the nervous system, for example, mutations in *MYO1C* are associated with bilateral hearing loss.[31 32] Given the known function of unconventional myosins, it is tempting to speculate that mutation of *MYO1H* impairs transport processes in neurons. With the exception of breathing deficits, we did not observe obvious autonomic nervous system abnormalities in the $Myo1h^{FS}$ or the *Myo1h** mice, but this might be due to their short survival periods which precluded further functional analyses. In-depth cellular analyses will be required to determine the precise role of *MYO1H* in the nervous system.

Acknowledgements We would like to thank the families for their collaboration and contribution to this project.

Contributors Patient recruitment and phenotyping: MS, IC, DEW-M, NL and SM; CRISPR experiments and mouse phenotyping: MS, LRH-M, BKK, IH and CB and SM; bioinformatics analyses: PK. All authors contributed in writing and reviewing the manuscript.

Funding This project was supported by grants from the Deutsche Forschungsgemeinschaft (DFG) to SM and CB. MS was supported by a grant from the DFG (SP1532/2-1) and by a fellowship of the Berlin-Brandenburg School for Regenerative Therapies, Berlin, Germany. LRH-M was supported by a grant from the European Commission under the scheme of Marie Skłodowska-Curie Intra-European fellowship (302477).

Competing interests None declared.

Patient consent Obtained.

Ethics approval The study was performed with the approval of the Charité Ethics Committee, Berlin, Germany.

Provenance and peer review Not commissioned; externally peer reviewed.

REFERENCES

1 Weese-Mayer DE, Berry-Kravis EM, Ceccherini I, Keens TG, Loghmanee DA, Trang H, Subcommittee A; ATS Congenital Central Hypoventilation Syndrome Subcommittee. An official ATS clinical policy statement: congenital central hypoventilation syndrome: genetic basis, diagnosis, and management. *Am J Respir Crit Care Med* 2010;181:626–44.
2 Carroll MS, Patwari PP, Kenny AS, Brogadir CD, Stewart TM, Weese-Mayer DE. Residual chemosensitivity to ventilatory challenges in genotyped congenital central hypoventilation syndrome. *J Appl Physiol*2014;116:439–50.
3 Weese-Mayer DE, Silvestri JM, Huffman AD, Smok-Pearsall SM, Kowal MH, Maher BS, Cooper ME, Marazita ML. Case/control family study of autonomic nervous system dysfunction in idiopathic congenital central hypoventilation syndrome. *Am J Med Genet* 2001;100:237–45.
4 Marazita ML, Maher BS, Cooper ME, Silvestri JM, Huffman AD, Smok-Pearsall SM, Kowal MH, Weese-Mayer DE. Genetic segregation analysis of autonomic nervous system dysfunction in families of probands with idiopathic congenital central hypoventilation syndrome. *Am J Med Genet* 2001;100:229–36.
5 Amiel J, Laudier B, Attié-Bitach T, Trang H, de Pontual L, Gener B, Trochet D, Etchevers H, Ray P, Simonneau M, Vekemans M, Munnich A, Gaultier C, Lyonnet S. Polyalanine expansion and frameshift mutations of the paired-like homeobox gene PHOX2B in congenital central hypoventilation syndrome. *Nat Genet* 2003;33:459–61.
6 Berry-Kravis EM, Zhou L, Rand CM, Weese-Mayer DE. Congenital central hypoventilation syndrome: phox2b mutations and phenotype. *Am J Respir Crit Care Med* 2006;174:1139–44.
7 Weese-Mayer DE, Berry-Kravis EM, Zhou L, Maher BS, Silvestri JM, Curran ME, Marazita ML. Idiopathic congenital central hypoventilation syndrome: analysis of genes pertinent to early autonomic nervous system embryologic development and identification of mutations in PHOX2b. *Am J Med Genet A* 2003;123A:267–78.
8 Weese-Mayer DE, Marazita ML, Rand CM, Berry-Kravis EM. Congenital central hypoventilation syndrome. In: Pagon RA, Adam MP, Ardinger HH, eds. Seattle (WA: GeneReviews(R)., 1993.
9 Rand CM, Yu M, Jennings LJ, Panesar K, Berry-Kravis EM, Zhou L, Weese-Mayer DE. Germline mosaicism of PHOX2B mutation accounts for familial recurrence of congenital central hypoventilation syndrome (CCHS). *Am J Med Genet A* 2012;158A:2297–301.
10 Bachetti T, Parodi S, Di Duca M, Santamaria G, Ravazzolo R, Ceccherini I. Low amounts of PHOX2B expanded alleles in asymptomatic parents suggest unsuspected recurrence risk in congenital central hypoventilation syndrome. *J Mol Med* 2011;89:505–13.
11 Dubreuil V, Ramanantsoa N, Trochet D, Vaubourg V, Amiel J, Gallego J, Brunet JF, Goridis C. A human mutation in Phox2b causes lack of CO2 chemosensitivity, fatal central apnea, and specific loss of parafacial neurons. *Proc Natl Acad Sci U S A* 2008;105:1067–72.
12 Borck G, Ur Rehman A, Lee K, Pogoda HM, Kakar N, von Ameln S, Grillet N, Hildebrand MS, Ahmed ZM, Nürnberg G, Ansar M, Basit S, Javed Q, Morell RJ, Nasreen N, Shearer AE, Ahmad A, Kahrizi K, Shaikh RS, Ali RA, Khan SN, Goebel I, Meyer NC, Kimberling WJ, Webster JA, Stephan DA, Schiller MR, Bahlo M, Najmabadi H, Gillespie

PG, Nürnberg P, Wollnik B, Riazuddin S, Smith RJ, Ahmad W, Müller U, Hammerschmidt M, Friedman TB, Riazuddin S, Leal SM, Ahmad J, Kubisch C. Loss-of-function mutations of ILDR1 cause autosomal-recessive hearing impairment DFNB42. *Am J Hum Genet* 2011;88:127–37.
13 Hussain MS, Baig SM, Neumann S, Peche VS, Szczepanski S, Nürnberg G, Tariq M, Jameel M, Khan TN, Fatima A, Malik NA, Ahmad I, Altmüller J, Frommolt P, Thiele H, Höhne W, Yigit G, Wollnik B, Neubauer BA, Nürnberg P, Noegel AA. CDK6 associates with the centrosome during mitosis and is mutated in a large Pakistani family with primary microcephaly. *Hum Mol Genet* 2013;22:5199–214.
14 Spielmann M, Brancati F, Krawitz PM, Robinson PN, Ibrahim DM, Franke M, Hecht J, Lohan S, Dathe K, Nardone AM, Ferrari P, Landi A, Wittler L, Timmermann B, Chan D, Mennen U, Klopocki E, Mundlos S. Homeotic arm-to-leg transformation associated with genomic rearrangements at the PITX1 locus. *Am J Hum Genet* 2012;91:629–35.
15 Borck G, Hög F, Dentici ML, Tan PL, Sowada N, Medeira A, Gueneau L, Holger T, Kousi M, Lepri F, Wenzeck L, Blumenthal I, Radicioni A, Schwarzenberg TL, Mandriani B, Fischetto R, Morris-Rosendahl DJ, Altmüller J, Reymond A, Nünberg P, Merla G, Dallapiccola B, Katsanis N, Cramer P, Kubisch C. BRF1 mutations alter RNA polymerase III-dependent transcription and cause neurodevelopmental anomalies. *Genome Res* 2015;25:155–66.
16 Kraft K, Geuer S, Will AJ, Chan WL, Paliou C, Borschiwer M, Harabula I, Wittler L, Franke M, Ibrahim DM, Kragesteen BK, Spielmann M, Mundlos S, Lupiáñez DG, Andrey G. Deletions, inversions, duplications: engineering of Structural variants using CRISPR/Cas in mice. *Cell Rep* 2015:833–9.
17 Artus J, Hadjantonakis AK. Generation of chimeras by aggregation of embryonic stem cells with diploid or tetraploid mouse embryos. *Methods Mol Biol* 2011;693:37–56.
18 Albrecht AN, Schwabe GC, Stricker S, Böddrich A, Wanker EE, Mundlos S. The synpolydactyly homolog (spdh) mutation in the mouse—a defect in patterning and growth of limb cartilage elements. *Mech Dev* 2002;112(1-2):53–67.
19 Chatonnet F, Wrobel LJ, Mézières V, Pasqualetti M, Ducret S, Taillebourg E, Charnay P, Rijli FM, Champagnat J. Distinct roles of Hoxa2 and Krox20 in the development of rhythmic neural networks controlling inspiratory depth, respiratory frequency, and jaw opening. *Neural Dev* 2007;2:19.
20 Brown SD, Moore MW. The International Mouse Phenotyping Consortium: past and future perspectives on mouse phenotyping. *Mamm Genome* 2012;23(9-10):632–40.
21 Menke DB, Guenther C, Kingsley DM. Dual hindlimb control elements in the Tbx4 gene and region-specific control of bone size in vertebrate limbs. *Development* 2008;135:2543–53.
22 Bongers EM, Duijf PH, van Beersum SE, Schoots J, Van Kampen A, Burckhardt A, Hamel BC, Losan F, Hoefsloot LH, Yntema HG, Knoers NV, van Bokhoven H. Mutations in the human TBX4 gene cause small patella syndrome. *Am J Hum Genet* 2004;74:1239–48.
23 Nimmakayalu M, Major H, Sheffield V, Solomon DH, Smith RJ, Patil SR, Shchelochkov OA. Microdeletion of 17q22q23.2 encompassing TBX2 and TBX4 in a patient with congenital microcephaly, thyroid duct cyst, sensorineural hearing loss, and pulmonary hypertension. *Am J Med Genet A* 2011;155A:418–23.
24 Kerstjens-Frederikse WS, Bongers EM, Roofthooft MT, Leter EM, Douwes JM, Van Dijk A, Vonk-Noordegraaf A, Dijk-Bos KK, Hoefsloot LH, Hoendermis ES, Gille JJ, Sikkema-Raddatz B, Hofstra RM, Berger RM. TBX4 mutations (small patella syndrome) are associated with childhood-onset pulmonary arterial hypertension. *J Med Genet* 2013;50:500–6.
25 Feldman JL, Mitchell GS, Nattie EE. Breathing: rhythmicity, plasticity, chemosensitivity. *Annu Rev Neurosci* 2003;26:239–66.
26 Wang H, Yang H, Shivalila CS, Dawlaty MM, Cheng AW, Zhang F, Jaenisch R. One-step generation of mice carrying mutations in multiple genes by CRISPR/Cas-mediated genome engineering. *Cell* 2013;153:910–8.
27 Spielmann M, Kakar N, Tayebi N, Leettola C, Nürnberg G, Sowada N, Lupiáñez DG, Harabula I, Flöttmann R, Horn D, Chan WL, Wittler L, Yilmaz R, Altmüller J, Thiele H, van Bokhoven H, Schwartz CE, Nürnberg P, Bowie JU, Ahmad J, Kubisch C, Mundlos S, Borck G. Exome sequencing and CRISPR/Cas genome editing identify mutations of ZAK as a cause of limb defects in humans and mice. *Genome Res* 2016;26:183–91.
28 Lupiáñez DG, Kraft K, Heinrich V, Krawitz P, Brancati F, Klopocki E, Horn D, Kayserili H, Opitz JM, Laxova R, Santos-Simarro F, Gilbert-Dussardier B, Wittler L, Borschiwer M, Haas SA, Osterwalder M, Franke M, Timmermann B, Hecht J, Spielmann M, Visel A, Mundlos S. Disruptions of topological chromatin domains cause pathogenic rewiring of gene-enhancer interactions. *Cell* 2015;161:1012–25.
29 Münnich S, Taft MH, Manstein DJ. Crystal structure of human myosin 1c—the motor in GLUT4 exocytosis: implications for Ca2+ regulation and 14-3-3 binding. *J Mol Biol* 2014;426:2070–81.
30 Tassopoulou-Fishell M, Deeley K, Harvey EM, Sciote J, Vieira AR. Genetic variation in myosin 1H contributes to mandibular prognathism. *Am J Orthod Dentofacial Orthop* 2012;141:51–9.
31 Adamek N, Geeves MA, Coluccio LM. Myo1c mutations associated with hearing loss cause defects in the interaction with nucleotide and actin. *Cell Mol Life Sci* 2011;68:139–50.
32 Lin T, Greenberg MJ, Moore JR, Ostap EM. A hearing loss-associated myo1c mutation (R156W) decreases the myosin duty ratio and force sensitivity. *Biochemistry* 2011;50:1831–8.